Modeling dermatophytosis in reconstructed human epidermis

Faway, Émilie; Cambier, Ludivine; Mignon, Bernard; Poumay, Yves; Lambert de Rouvroit, Catherine

Published in:
Medical mycology

DOI:
10.1093/mmy/myw111

Publication date:
2016

Document Version
Peer reviewed version

Full title:

Modeling dermatophytosis in reconstructed human epidermis: a new tool to study infection mechanisms and to test antifungal agents

Short title:

***In vitro* model of human dermatophytosis**

Émilie Faway[1], Ludivine Cambier[2], Bernard Mignon[2], Yves Poumay[1] and Catherine Lambert de Rouvroit[1]

[1] URPHYM-NARILIS, University of Namur, Namur, Belgium

[2] FARAH, Faculty of Veterinary Medicine, University of Liège, Liège, Belgium

Correspondence: Professor Yves Poumay, Cell and Tissue Laboratory, URPHYM-NARILIS, University of Namur, 61, rue de Bruxelles, B-5000 Namur, Belgium.

E-mail: yves.poumay@unamur.be

Phone: +32 81 72 42 57

Keywords

- Dermatophytosis
- Reconstructed Human Epidermis
- Model of infection
- *Trichophyton rubrum*
- Miconazole

Abstract

Dermatophytosis is a superficial fungal infection of keratinized structures that exhibits an increasing prevalence in humans and is thus requesting novel prophylactic strategies and therapies. However, precise mechanisms used by dermatophytes to adhere at the surface of the human epidermis and invade its *stratum corneum* are still incompletely identified, as well as the responses provided by the underlying living keratinocytes during the infection. We hereby report development of an *in vitro* model of human dermatophytosis through infection of reconstructed human epidermis (RHE) by arthroconidia of the anthropophilic *Trichophyton rubrum* species or of the zoophilic *Microsporum canis* and *Arthroderma benhamiae* species. By modulating density of conidia in the inoculum and duration of exposure to such pathogens, fungal infection limited to the *stratum corneum* was obtained, mimicking severe but typical *in vivo* situation. Fungal elements in infected RHE were monitored over time by histochemical analysis using Periodic-Acid Schiff-staining or quantified by qPCR-detection of fungal genes inside RHE lysates. This model brings improvements to available ones, dedicated to better understand how dermatophytes and epidermis interact, as well as to evaluate preventive and therapeutic agents. Indeed, miconazole topically added to RHE was demonstrated to inhibit fungal infection in this model.

Introduction

Dermatophytosis is a superficial infection of keratinized structures of the host due to several species of keratinolytic fungi named dermatophytes. *In vivo*, infection of human glabrous skin by dermatophytes is limited to the *stratum corneum* [1], except in immunosuppressed patients where fungal elements can be observed in deeper tissues [2-4]. Absence of immune cells and serum inside the *stratum corneum*, as well as the presence of tight junctions between keratinocytes of the *stratum granulosum*, might explain why dermatophytes remain localized in the superficial epidermal layer [5]. Prevalence of dermatophytosis is estimated around 20% in the global human population but is increasing for the last decade in industrialized countries, principally due to immigration and travel, as well as to more frequent sport activities, marked aging of the population and rising incidence of both diabetes and vascular diseases [6]. Among the numerous species of dermatophytes referred as being able to infect humans, the anthropophilic *Trichophyton rubrum* species is responsible for more than 90% of human lesions [7,8].

Despite their threatening prevalence, information is still lacking about mechanisms used by dermatophytes to adhere [9,10] and invade [11,12] host tissues, as well as about specific responses adopted by keratinocytes present in the underlying living layers in order to alert the immune system and fight against these pathogens. In addition, the current availability of effective drugs for the treatment of human dermatophytosis is rather limited. Although most human lesions can be treated locally, other require systemic treatment, due to their extent or poor accessibility for a topical treatment of the lesion. Furthermore, treatment with systemic drugs remains expensive and often associated with potential toxicity, and must cope with the emergence of drug-resistance [13,14]. Finally, patients who suffer from epidermal lesions caused

by dermatophytes are often subject to recurrence after primary infection. Taken together, the problems associated with currently available treatments raise the need for developing novel preventive and curative strategies and compounds against dermatophytes.

In order to gain knowledge about the pathogenesis of dermatophytosis, as well as to perform safe and relevant *in vitro* efficacy testing for innovative preventive strategies or new fungicidal compounds, modeling dermatophytosis in a model based on *in vitro* reconstructed human epidermis (RHE) appears as a valuable tool for basic and preclinical studies.

Several models of dermatophytosis have been previously proposed such as stripped sheet of *stratum corneum* [15], nails or hairs samples [16], or epidermal cell cultures prepared as monolayers [17,18]. *Ex vivo* infection models of human skin explants by dermatophytes have also been developed to evaluate fungal growth [19,20], mechanisms of adhesion [9] and modulation of gene expression [21] during infection. However, all those models present serious limitations. On one hand, stripped sheets of *stratum corneum*, like nails and hairs, do not contain any living keratinocytes and therefore impede evaluation of eventual responses of host to infection. On the other hand, monolayers of cultured keratinocytes cannot proceed to keratinization although the process is required to analyze dermatophytosis and mechanisms involved in its pathogenesis. Finally, the use of human skin explants is limited due to restricted availability and variability between samples (thickness, hairiness). Recently, cultured skin equivalents were used to overcome such limitations and appeared relevant to mimic lesions caused by the disease [22-24] and to test the efficacy of antifungal molecules [25,26].

RHE can be produced from cultured normal human keratinocytes, seeded at high density onto a polycarbonate filter, fed from the lower compartment, and exposed to air-liquid interface in order to induce keratinization and formation of the cornified barrier. RHE have been

characterized to be morphologically and functionally similar enough to the human epidermis in order to become relevant tools for studies of physiological and pathological features of this tissue[27-29]. In addition, RHE were demonstrated suitable for the characterization of keratinocyte responses to chemical compounds, either irritant or sensitizer, layered onto the *stratum corneum* [30].

In this study, this RHE model was evaluated to study *in vitro* infection by anthropophilic dermatophyte *T. rubrum* as well as by zoophilic *Microsporum canis* or *Arthroderma benhamiae* species. Mechanisms involved in fungal infection, such as adhesion of conidia, invasion and proliferation of dermatophytes, were investigated, as well as responses induced in the hosting epidermis. Finally, proving efficacy of miconazole in such a model has started paving a way for testing newly developed antifungal agents.

Materials and Methods

Dermatophyte strains and production of arthroconidia

Three different strains of *T. rubrum* were used in this study, namely IHEM 13894, IHEM 13809 and IHEM 13886 as well as strain IHEM21239 of *M. canis* and strain IHEM20163 of *A. benhamiae*. Strains of *T. rubrum* and *A. benhamiae* were isolated from naturally infected human skin, while *M. canis* strain was isolated from naturally infected cat hair. All these strains were obtained from the Belgian Co-ordinated Collections of Micro-organisms (BCCM/IHEM collection of biomedical fungi and yeasts, Brussels).

Arthroconidia were produced as previously described [22]. Briefly, fungi were grown on Sabouraud dextrose agar at 27°C for three weeks to reach confluency of the cultures. Fungal

material was then scraped, cut into small pieces and seeded over 2% yeast extract/1% peptone (YEN) agar. After approximately two weeks of culture on YEN agar at 30°C in an atmosphere containing 12% CO_2, surface mycelium was scraped, cut into small pieces again and added to sterile Phosphate-Buffered Saline (PBS). This solution was stirred for two hours at 4°C and then filtered through three Miracloth layers (22-25 µm pore size; Millipore cat. no. 475855) in order to recover unicellular fungal elements corresponding to arthroconidia. The culture plates were observed under the microscope during the production process for the obtention of arthroconidia and microconidia were never observed. The concentration of arthroconidia was determined by seeding the prepared solution onto Sabouraud dextrose agar and counting colony-forming units (CFU) after seven days of growth at 27°C. Arthroconidia were stored at 4°C and used within one month.

Reconstructed human epidermis and culture media

RHE were prepared as previously described [27]. In brief, normal human keratinocytes were isolated from adult skin samples obtained at plastic surgery (Dr. Bienfait, Clinique St. Luc, Namur-Bouge, Belgium). Third passage keratinocytes were seeded onto polycarbonate culture inserts (0.4 µm pore size; Millipore cat. no. PIHP01250) at a density of 250,000 cells/cm² in EpiLife medium (Invitrogen-Cascade Biologics™ cat. no. M-EPI-500-CA) supplemented with Human Keratinocyte Growth Supplement (HKGS; Invitrogen-Cascade Biologics™ cat. no. S-001-5) and containing 1.5 mM Ca^{2+} concentration. After 24 h, keratinocytes were exposed to the air-liquid interface by carefully removing culture medium above the filter, while the medium under the filter was replaced by EpiLife medium supplemented with HKGS, 1.5 mM Ca^{2+}, 10 ng/ml keratinocyte growth factor (KGF; R&D

systems cat. no. 251-KG) and 50 µg/ml vitamin C. The medium was then changed every two days. Fully differentiated RHE were obtained eleven days after seeding. Infected RHE were also cultured in EpiLife medium supplemented with HKGS, 1.5 mM Ca^{2+}, 10 ng/ml KGF and 50 µg/ml vitamin C.

Histological processing and staining

For histology, RHE were fixed by incubation for 24 hours in 4% formaldehyde solution, dehydrated in methanol, and then incubated in toluene before embedding in paraffin. Tissue sections (6 µm thickness) were prepared perpendicular to the polycarbonate filter. Then sections were deparaffinized, rehydrated, rinsed with water and finally stained. Periodic-Acid Schiff (PAS) staining was then performed, using hemalun for counterstaining as in standard protocols.

In order to degrade intracellular glycogen, tissue sections were deparaffinized, rehydrated, rinsed with water and incubated for one hour in 0.1% α-amylase from porcine pancreas (Sigma cat. no. A3176) dissolved in PBS solution, prior to PAS-staining and hemalun counterstaining as usual.

DNA extraction

For total DNA extraction, infected RHE previously frozen at -80°C were homogenized using Tissue Grinder (NIPPON Genetics EUROPE cat. no. NG010). DNeasy® Blood & Tissue Kit (Qiagen cat. no. 69504) was used for isolation and purification of total DNA from tissue, according to the manufacturer's instructions.

Primer specificity and standard curve for quantitative PCR (qPCR)

For amplification of the gene sequence corresponding to *T. rubrum* 18S rDNA gene (*Tr* 18S), primers 18SrDNA-F (5'-TAACGAACGAGACCTTAACC-3') and 18SrDNA-R (5'-TTATTGCCTCAAACTTCCAT-3'), previously described by Paugam *et al*. [31], were used. Amplification mixture was composed of 30 ng total DNA extracted from infected or control RHE, 0.3 mM dNTP, 50 mM $MgSO_4$, 1X *Pfx* amplification buffer, one unit Platinum *Pfx* DNA polymerase (Invitrogen cat. no. 11708-013) and 300 nM of each primer in a total volume of 50 µl. Amplification program was 5 min denaturation at 94°C, 40 cycles of denaturation for 30 sec at 94°C, annealing for 30 sec at 60°C and elongation for 45 sec at 68°C with a final elongation step of 10 min at 68°C. Amplification products were electrophoresed on agarose gels, stained with ethidium bromide, and observed under ultraviolet illumination. Primers specificity was confirmed by obtaining a unique PCR product of expected molecular size after DNA analysis from pure *T. rubrum* mycelium, after analysis from infected RHE, but not after analysis of DNA extracted from non-infected RHE.

A standard curve of known *Tr* 18S rDNA copy number was required for absolute quantification of infection using quantitative PCR. *Tr* 18S rDNA was amplified from DNA extracted from infected RHE as described above and purified using MinElute® PCR Purification Kit (Qiagen cat. no. 28004), according to the manufacturer's instructions. Subsequently, the concentration of purified product was measured using a NanoDrop 1000 Spectrophotometer (Thermo Scientific) and *Tr* 18S rDNA copy number was calculated using Avogadro's number. Concentration was adjusted to 10^{10} *Tr* 18S rDNA copies/ µl and standard curve was obtained by serial dilution from 10^8 down to 10^1 *Tr* 18S rDNA copies/µl.

Absolute quantification by qPCR

PCR mixture was composed of Takyon™ ROX SYBR® Master Mix (Eurogentec cat. no. UF-RSMT-B0701), 300 nM of 18SrDNA-F primer, 300 nM of 18SrDNA-R primer and 20 ng of DNA in a total volume of 15 µl. The amplification protocol involved 10 min of denaturation at 95°C followed by 45 cycles of denaturation for 10 sec at 95°C, annealing for 10 sec at 60°C and elongation for 10 sec at 72°C. Absolute quantification was performed according to standard curve of serial dilution from 10^8 down to 10^1 *Tr* 18S rDNA copies/µl.

Measurement of RHE viability using MTT assay

In this study, MTT assay was performed in order to assess the effect of miconazole or dimethyl-sulfoxide (DMSO), which is the solvent of miconazole, on cellular viability in the RHE. In practice, RHE were incubated for four hours in presence of miconazole or its solvent, then incubated for one hour with 0.5 mg/ml of tetrazolium dye MTT (Sigma cat. no. M5655). RHE were then transferred for 30 min in isopropanol to solubilize and homogenize formazan produced inside living keratinocytes, and the optical density of the solution was determined at 540 nm using a VersaMax Microplate Reader spectrophotometer (Molecular Devices).

Statistical Analyses

All statistical analyses were carried out using GraphPad Prism 5 software. One-way analysis of variance (ANOVA1) were performed to analyze our data. A *P* value of 0.05 or less was taken as being significant.

Results

Infection of RHE using *T. rubrum* arthroconidia

RHE were infected on the 11th day of reconstruction, when their morphological and functional features were becoming similar to those of the human epidermis *in vivo* [29]. For infection, *T. rubrum* IHEM 13894 arthroconidia, in suspension in PBS, were topically applied on the top of RHE. Several inoculum sizes were tested in order to determine the amount of arthroconidia required to initiate an infection limited to the cornified layer, as observed *in vivo*. The density chosen to inoculate RHE was 1,700 arthroconidia per cm². Four hours after inoculation, fungal suspension was eliminated and three washes with PBS were performed in order to remove non-adherent arthroconidia and to expose keratinocytes to the air-liquid interface again. Then, infected RHE were maintained at 37°C in a humidified atmosphere containing 5% CO_2 for four additional days with culture medium changed every day. Samples were then collected and processed for histological analysis.

PAS staining was used to detect dermatophytes in sections of infected RHE. Indeed, this histochemical procedure highlights polysaccharides, such as chitin, which is the main component of fungal cell wall. However supra-basal keratinocytes inside RHE were surprisingly stained after the PAS staining. Pretreatment of RHE sections with α-amylase, an enzyme which digests glycogen, proved that this staining in keratinocytes actually corresponds to glycogen accumulation (**Figure 1A**). Thus, α-amylase pretreatment has been systematically performed before PAS staining in all subsequent experiments in order to improve specificity of fungal detection using this technique.

During the four days following inoculation, morphological analysis of infected RHE revealed that arthroconidia proliferated over time and progressively invaded the *stratum corneum* of the RHE without reaching layers containing living keratinocytes, as it usually happens during *in vivo* infection. From the fifth day after inoculation, fungal elements started to invade layers composed of living keratinocytes, leading to severe tissue damage (**Figure 1B**).

To validate our model, we infected RHE with arthroconidia from two other strains of *T. rubrum*, namely IHEM 13809 and IHEM 13886 strains, using the same procedure. Staining of infected RHE four days after inoculation, showed that arthroconidia from the different *T. rubrum* strains invade RHE in a similar manner (**Figure 1C**).

In addition, we adapted this infection model to other dermatophyte species. RHE were infected with arthroconidia from *M. canis* IHEM 21239 or from *A. benhamiae* IHEM 20163 using the procedure described above. Different sizes of inoculum were tested in order to determine the number of arthroconidia requested to develop infection similar to that obtained with *T. rubrum*. Inoculation by arthroconidia of *M. canis* or of *A. benhamiae*, at a density of respectively 17,000 and 53 per cm^2, induced infection which remained limited to the cornified layer at the fourth day following the inoculation (**Figure 1C**). Those results suggest that this model could be adapted to study epidermal infection by other species.

All subsequent experiments were performed using arthroconidia from *T. rubrum* IHEM 13894 strain.

Quantification of infection by qPCR of *T. rubrum* 18S rDNA gene

We established a PCR-based method to quantify the infection of RHE by *T. rubrum* arthroconidia. Total DNA was extracted from infected RHE one, two, three and four days after inoculation and the copy number of *Tr* 18S rDNA was assessed by qPCR using a standard curve consisting in samples of known *Tr* 18S rDNA copy number. DNA extracted from non-infected RHE served as negative control.

Tr 18S rDNA copy number progressively increased during the four days following the inoculation corresponding to 38 ± 7, 871 ± 329, 24.704 ± 11.605 and 52.532 ± 24.523 respectively (**Figure 2**). This quantification was performed three times using RHE produced with keratinocytes isolated from three different donors, likely explaining the observed variability.

Adhesion kinetics of *T. rubrum* arthroconidia to RHE

Adhesion kinetics of *T. rubrum* arthroconidia to RHE was studied by CFU counting. To perform this analysis, RHE inoculated with 1,700 *T. rubrum* arthroconidia per cm² were washed with PBS after 0, 1, 2, 4, 6 or 24 hours following inoculation. Non-adherent arthroconidia recovered in the solution used for these washes were seeded on Sabouraud dextrose agar and grown at 27°C for seven days. Numbers of CFU, corresponding to the number of non-adherent arthroconidia, were counted and subtracted from the number of arthroconidia inoculated on RHE in order to calculate the percentage of adherent arthroconidia. Percentage of adherent arthroconidia increased in accordance with duration of contact with RHE, starting from 1% only when RHE were rinsed immediately, but reaching 91% when contact duration was 24 hours (**Figure 3A**).

Four days after inoculation, the histological analysis of RHE also revealed that the extent of invasion by arthroconidia increased with duration of contact (**Figure 3B**).

Miconazole inhibits infection of RHE by *T. rubrum* arthroconidia

Inhibitory activity of miconazole [32] was assessed on the RHE model of infection described above.

Firstly, minimum inhibitory concentration (MIC) of miconazole, defined as the lowest concentration able to prevent growth of *T. rubrum* arthroconidia, was determined. For this purpose, *T. rubrum* arthroconidia were seeded on Sabouraud dextrose agar in presence of miconazole at concentration ranging from 0.4 µg/ml to 6.4 µg/ml. Arthroconidia were grown during seven days at 27°C and then CFU were counted. Percentage of growth was determined as the percentage of seeded arthroconidia that have formed a colony. This percentage of growth was 100% in absence of miconazole and decreased in a dose-dependent manner in presence of miconazole (**Figure 4A**). At a concentration of 3.2 µg/ml, the percentage of growth dropped down to 0%, suggesting that 3.2 µg/ml was the MIC of miconazole. As a negative control, a PBS solution containing 6.4% DMSO, which is the highest concentration of the miconazole solvent, was found unable to alter *T. rubrum* growth.

A MTT assay demonstrated that, neither miconazole nor PBS solution containing DMSO, could alter keratinocyte survival (**Figure 4B**).

Finally, inhibitory effect of miconazole was checked using our model of RHE infection by *T. rubrum* arthroconidia. Two experimental settings were carried out. On one hand, miconazole was topically applied on RHE simultaneously with arthroconidia. On the second hand, miconazole was topically added on infected RHE one day after being inoculated with

arthroconidia. In both experimental settings, RHE were exposed to air-liquid interface again four hours after miconazole application. RHE infected in the presence of miconazole were then processed for histological analysis four days after inoculation and compared with infected RHE cultured in absence of miconazole. In both experimental settings, miconazole effectively inhibited the infection of RHE by *T. rubrum* arthroconidia, as evidenced by the absence of fungal elements in the *stratum corneum*, four days after inoculation of RHE (**Figure 4C**). This result was confirmed by a huge decrease in *Tr* 18S rDNA copy numbers in presence of miconazole, measured by qPCR after total DNA extraction from infected RHE four days after inoculation (**Figure 4C**). An additional experimental setting was carried out in order to assess the efficacy of miconazole on previously infected RHE. Miconazole was topically applied on infected RHE four days after inoculation with arthroconidia, and reapplied each day up to the seventh day following inoculation. RHE were exposed to air-liquid interface again four hours after each miconazole application and were finally processed for histological analysis eight days after inoculation. Miconazole was able to stop the infection process, as shown by the limited extent of fungal invasion (**Figure 4D**). This was confirmed by measurement of *Tr* 18S rDNA copy numbers by qPCR after total DNA extraction from infected RHE eight days after inoculation (**Figure 4D**).

Discussion

In this study, a model of dermatophytosis on RHE using the *T. rubrum* anthropophilic species, responsible for the majority of human infections, has been developed. A density of 1,700 arthroconidia per cm^2 allows infection of *stratum corneum* without invasion of deeper layers made of living keratinocytes during the four days following inoculation, as it happens *in vivo*

in infected glabrous human skin. Obviously, infection of RHE becomes more severe than *in vivo* where only a few fungal elements are dispersed in the *stratum corneum*. As RHE in this model completely lack immune cells and serum, keratinocytes alone react to counteract the progression of arthroconidia into the living layers of the epidermis. Taking these parameters into account, the experimental conditions were chosen in order to obtain a significant infection, thereby facilitating the study of dermatophytosis pathogenesis and keratinocyte responses. Thus, this model seems representative of *in vivo* human skin infection by *T. rubrum* and is validated using three different strains of this species.

In addition, the model was adapted for two other dermatophyte species, namely *M. canis* and *A. benhamiae*, by adapting the initial number of arthroconidia used to infect RHE. Interestingly, the suitable size of inoculum varied considerably between species: 1,700 arthroconidia per cm^2 for *T. rubrum*, 17,000 for *M. canis* and 53 for *A. benhamiae*. Such a huge difference might potentially reflect variability in the processes involved during infection. Firstly, upon contact with host tissue components, different strains of pathogenic fungi express different adhesin genes. Moreover, different alleles encode adhesin proteins with variable number of tandem repeats, and in turn different adhesion properties, as shown for instance in clinical isolates of *C. albicans* [33]. In *T. rubrum*, an adhesin-like protein with a tandem repeat pattern was recently reported as induced in conidia grown on keratin [34]. Interestingly, homologous proteins with variable numbers of tandem repeats are found in different dermatophyte species, including *M. canis* and *A. benhamiae*. Secondly, other components involved in the host-pathogen interaction could be responsible for the difference in the number of fungal elements necessary to trigger infection, namely protease expression level and activity which are characteristic of individual dermatophyte species cultured *in vitro* [35]. Thirdly, the difference in suitable inoculum size maybe reflects that the level of *in vivo* human

skin infection is species-dependent, zoophilic species being more inflammatory than anthropophilic ones [36,37]. Notably, *A. benhamiae* causes highly inflammatory human lesions, in good accordance with the *in vitro* observation that a small number of arthroconidia is sufficient to induce infection of RHE comparable to RHE infection by *T. rubrum*. Anyhow, these results suggest that infection model of RHE can easily be adapted to other dermatophyte species by modulating the size of inoculum.

Recently, two infection models by *T. rubrum* dermatophytes on living skin equivalent were reported. Firstly, Achterman *et al*. [23] infected commercially available EpiDerm tissues with conidia from *T. rubrum* as well as with four other different dermatophytes species (*T. tonsurans*, *T. equinum*, *M. canis* and *M. gypseum*). However, the size of inoculum was chosen in that report on the basis of lactate dehydrogenase release in the culture medium of infected tissues as an indication of tissue damages. Since no morphological analysis was performed, the extent of infection has not been assessed. In addition, an equal number of conidia was used to infect tissues, irrespective of the species involved, whereas it is well known that the level of human skin infection is highly species-dependent [36,37]. Notably zoophilic species, such as *M. gypseum*, give rise to more inflammatory lesions than anthropophilic fungi, like *T. rubrum* for instance. In another model, Liang *et al*. [24] used available commercial epidermal tissue EpiSkin to mimic human infection by *T. rubrum*. In that study, the authors have assessed tissues invasion by means of histological analysis. A drawback of those two models is the use of conidia as infecting fungal elements. These conidia are either pluricellular macroconidia or, more likely, unicellular microconidia. Both are saprophytic elements which are produced by anthropophilic dermatophytes exclusively in culture, and which have never been observed in dermatophytosis lesions *in vivo*. Oppositely, in the present model, the use of arthroconidia is more representative of *in vivo* infecting spores [38].

Further specificity was brought to RHE histological analysis by performing α-amylase pretreatment before proceeding to standard PAS-staining. Indeed suprabasal keratinocytes are highlighted by PAS staining in this model, but also in the two published models, due to yet unexplained presence of glycogen. This background signal is effectively eliminated by α-amylase treatment but was not taken into account in the previous studies [23,24].

In addition, a method based on qPCR to quantify the infection of RHE by dermatophytes has been developed herein. PCR methods are already used for detection of dermatophytes in diagnosis of human infection [31,39,40], but to our knowledge, absolute quantitation of infection has never been performed so far. This method allows to quantitatively evaluate the progression of infection by *T. rubrum* arthroconidia during the four days following inoculation of RHE. Furthermore, this method will nowadays be used as a sensitive measuring procedure, relevant to compare levels of adhesion and infection between different species and/or in different conditions, thus allowing assessment of the efficacy of putative antifungal compounds.

Adhesion kinetics of arthroconidia to RHE was assessed by CFU counting method. As expected, percentage of adherent arthroconidia increases according to the duration of contact. Accordingly, the analysis of infected RHE four days after inoculation revealed that the extent of infection is related to duration of contact between arthroconidia and tissue. Adhesion increases significantly after one hour, suggesting that it constitutes an early step of infection in accordance with previous studies [15,41]. Even in RHE which were rinsed immediately after inoculation, morphological analysis revealed the presence of some fungal elements four days later. This could mean either that adhesion is an immediate process, or that washing procedure does not remove all arthroconidia from the RHE. However, no significant

differences are observed between percentages of adherent arthroconidia after one, two and four hours of contact with RHE, indicating that at least six hours are needed to reach high levels of adhesion.

Finally, the efficacy of miconazole in inhibiting the infection of RHE by *T. rubrum* arthroconidia was confirmed by morphological and qPCR analyses. These results prove that this model is a valid tool to assess the efficiency of new potential anti-dermatophyte compounds. In the past, dermatophytosis models on skin equivalent were already used to test the efficacy of antifungal agents [25,26]. In those studies, antifungal molecules were added in culture media of reconstructed epidermis to mimic systemic administration. On the contrary, miconazole was hereby topically applied on the *stratum corneum*. In the current context, where new drugs against dermatophytosis are requested, the development of a human model allowing efficiency tests of topical therapeutic or preventive novel agents is highly relevant.

In summary, a dermatophytosis model on RHE and two methods to quantify infection have been successfully developed. These tools allow the study of direct interactions between dermatophytes and keratinocytes as well as the evaluation of efficacy for putative antifungal agents. However RHE, as other skin equivalent models, present several unavoidable limitations. Indeed, absence of skin appendages, sebum, cutaneous microflora and immune system makes RHE more susceptible to fungal infection than *in vivo* human skin. Consequently, analysis of infected RHE in our model occurs four days after inoculation, well before dermatophytes start to invade layers of living keratinocytes and finally destroy the full epidermis. Despite these limitations, the present model brings improvements to already available tools dedicated to better understanding epidermal involvements of dermatophytes, as well as to evaluate novel preventive or therapeutic antifungal agents.

Acknowledgements

The authors gratefully acknowledge the technical help provided by B. Balau, V. De Glas, K. De Swert and D. Van Vlaender. Special thanks are addressed to Dr B. Bienfait (Clinique St. Luc, Namur-Bouge, Belgium) for providing skin samples. EF is supported by a research fellowship (MYCAVERT, convention 1318058) from the *Région Wallonne*.

Conflict of interest

None.

References

1. Weitzman I, Summerbell R. The dermatophytes. *Clin Microbiol Rev*. 1995; **8**: 240-259
2. Smith K, Welsh M, Skelton H. *Trichophyton rubrum* showing deep dermal invasion directly from the epidermis in immunosuppressed patients. *Br J Dermatol*. 2001; **145**: 344-348
3. Cheng C, Hsiao Y, Ko. J. Disseminated deep dermatophytosis caused by *Trichophyton rubrum*. *Dermatol Sin*. 2014; **32**: 191-192
4. Squeo R, Beer R, Silvers D, Weitzman I, Grossman M. Invasive *Trichophyton rubrum* resembling blastomycosis infection in the immunocompromised host. *J Am Acad Dermatol*. 1998; **39**: 379-380
5. Carlisle D, Inouye J, King R, Jones H. Signifiance of serum fungal inhibitory factor in dermatophytosis. *J Invest Dermatol*. 1974; **63**: 239-241
6. Havlickova B, Czaika V, Friedrich M. Epidemiological trends in skin mycoses worldwide. *Mycoses*. 2008; **51**: 2-15

7. Seebacher C, Bouchara J-P, Mignon B. Updates on the epidemiology of dermatophyte infections. *Mycopathologia*. 2008; **166**: 335-352

8. Nenoff P, Krüger C, Ginter-Hanselmayer G, Tietz H. Mycology- an update. Part 1: dermatomycoses: causative agents, epidemiology and pathogenesis. *J Dtsch Dermatol Ges*. 2014; **1610-0379**: 188-205

9. Bagut E, Baldo A, Mathy A, et al. Subtilisin Sub3 is involved in adherence of *Microsporum canis* to human and animal epidermis. *Vet Microbiol*. 2012; **160**: 413-419

10. Baldo A, Chevigné A, Dumez M, et al. Inhibition of the keratinolytic subtilisin protease Sub3 from *Microsporum canis* by its propeptide (proSub3) and evaluation of the capacity of proSub3 to inhibit fungal adherence to feline epidermis. *Vet Microbiol*. 2012; **159**: 479-484

11. Baldo A, Mathy A, Tabart J, et al. Secreted subtilisin Sub3 from *Microsporum canis* is required for adherence to but not for invasion of the epidermis. *Br J Dermatol*. 2010; **162**: 990-997

12. Baldo A, Monod M, Mathy A, et al. Mechanisms of skin adherence and invasion by dermatophytes. *Mycoses*. 2012; **55**: 218-223

13. Osborne C, Leitner I, Favre B, Ryder N. Amino acid substitution in *Trichophyton rubrum* epoxidase associated with resistance to terbinafine. *Antimicrob Agents Chemother*. 2005; **49**: 2840-2844

14. Mukherjee P, Leidich S, Isham N, Leitner I, Ryder N, Ghannoum M. Clinical *Trichophyton rubrum* strain exhibiting primary resistance to terbinafine. *Antimicrob Agents Chemother*. 2003; **47**: 82-86

15. Zurita J, Hay R. Adherence of dermatophyte microconidia and arthroconidia to human keratinocytes *in vitro*. *J Invest Dermatol*. 1987; **89**: 529-534

16. Grumbt M, Monod M, Yamada T, Hertweck C, Kunert J, Staib P. Keratin degradation by dermatophytes relies on dioxygenase and sulfite efflux pump. *J Invest Dermatol*. 2013; **133**: 1550-1555

17. Nakamura Y, Kano R, Hasegawa A, Watanabe S. Interleukin-8 and tumor necrosis factor alpha production in human epidermal keratinocytes induced by *Trichophyton mentagrophytes*. *Clin Diagn Lab Immunol*. 2002; **9**: 935-937

18. Shiraki Y, Ishibashi Y, Hiruma M, Nishikawa A, Ikeda S. Cytokine secretion profiles of human keratinocytes during *Trichophyton tonsurans* and *Arthroderma benhamiae* infections. *J Med Microbiol*. 2006; **55**: 1175-1185

19. Duek L, Kaufman G, Ulman Y, Berdicevsky I. The pathogenesis of dermatophyte infections in human skin sections. *J Infect*. 2004; **48**; 175-180

20. KaufmanG, Horwitz B, Duek L, Ullman Y, Berdicevsky I. Infection stages of the dermatophyte pathogen *Trichophyton*: microscopic characterization and proteolytic anzymles. *Med Mycol*. 2007; **45**; 149-155

21. Peres N, da Silva L, da Silva Santos R, et al. *In vitro* and *ex vivo* infection models help assess the molecular aspects of the interaction of *Trichophyton rubrum* with the host milieu. *Med Mycol*. 2016; **54**; 420-427

22. Tabart J, Baldo A, Vermout S, et al. Reconstructed interfollicular feline epidermis as a model for *Microsporum canis* dermatophytosis. *J Med Microbiol*. 2007; **56**: 971-975

23. Achterman R, Moyes D, Thavaraj S, et al. Dermatophytes activate skin keratinocytes via mitogen-activated protein kinase signaling and induce immune responses. *Infect Immun*. 2015; **83**: 1705-1714

24. Liang P, Huang X, Yi J, et al. A *Trichophyton rubrum* infection model based on the reconstructed human epidermis – Episkin®. *Chin Med J.* 2016; **129**: 54-58

25. Rashid A, Edward M, Richardson M. Activity of terbinafine on *Trichophyton mentagrophytes* in human living skin equivalent model. *J Med Vet Mycol*. 1995; **33**: 229-233

26. Tabart J, Baldo A, Vermout S, Losson B, Mignon B. Reconstructed interfollicular feline epidermis as a model for the screening of antifungal drugs against *Microsporum canis*. *Vet Dermatol.* 2008 ; **19**: 130-133

27. De Vuyst E, Charlier C, Giltaire S, De Glas V, Lambert de Rouvroit C, Poumay Y. Reconstruction of normal and pathological human epidermis on polycarbonate filtre. *Methods Mol Biol*. 2014; **1195**: 191-201

28. Poumay Y, Dupont F, Marcoux S, Leclercq-Smekens M, Hérin M, Coquette A. A simple reconstructed human epidermis: preparation of the culture model and utilization in *in vitro* studies. *Arch Dermatol Res*. 2004; **296**: 203-211

29. Frankart A, Malaisse J, De Vuyst E, Minner F, Lambert de Rouvroit C, Poumay Y. Epidermal morphogenesis during progressive *in vitro* 3D reconstruction at the air-liquid interface. *Exp dermatol*. 2012; **21**: 871-875

30. Frankart A, Coquette A, Schroeder K-R, Poumay Y. Studies of cell signaling in a reconstructed human epidermis exposed to sensitizers: IL-8 synthesis and release depend on EGFR activation. *Arch Dermatol Res*. 2012; **304**: 289-303

31. Paugam A, L'Ollivier C, Viguié C, et al. Comparison of real-time PCR with conventional methods to detect dermatophytes in samples from patients with suspected dermatophytosis. *J Microbiol Methods*. 2013; **95**: 218-222

32. Barasch A, Voinea Griffin A. Miconazole revisited: new evidence of antifungal efficacy from laboratory and clinical trials. *Future Microbiol*. 2008; **3**: 265-269

33. Verstrepen K, Klis F. Flocculation, adhesion and biofilm formation in yeasts. *Mol Microbiol*. 2006; **60**: 5-15

34. Bitencourt, T, Macedo, C, Franco M, et al. Transcription profile of *Trichophyton rubrum* conidia grown on keratin reveals the induction of an adhesin-like protein gene with a tandem repeat pattern. *BMC Genom*. 2016; **17**: 249

35. Giddey, K, Frave, B, Quadroni, M, Monod, M. Closely related dermatophyte species produce different patterns of secreted proteins. *FEMS Microbiol Lett*. 2006; **267**: 95-101

36. Noguchi H, Jinnin M, Miyata K, Hiruma M, Ihn H. Clinical features of 80 cases of *tinea faciei* treated at a rural clinic in Japan. *Drug Discov Ther*. 2014; **8**: 245-248

37. Degreef H. Clinical forms of dermatophytosis (ringworm infection). *Mycopathologia*. 2008; **166**: 257-265

38. Rashid A. Arthroconidia as vector of dermatophytosis. *Cutis* 2001; **67**

39. Dhib I, Fathallah A, Charfeddine I, et al. Evaluation of Chitine synthase (CHS1) polymerase chain reaction assay in diagnosis of dermatophyte onychomycosis. *J Mycol Med*. 2012; **22**: 249-255

40. Ohst T, Kupusch C, Gräser Y. Detection of common dermatophytes in clinical specimens using a simple quantitative real-time TaqMan PCR assay. *Br J Dermatol*. 2015; **174**: 602-609

41. Baldo A, Tabart J, Vermout S, et al. Secreted subtilisins of *Microsporum canis* are involved in adherence of arthroconidia to feline corneocytes. *J Med Microbiol*. 2008; **57**: 1152-1156

Legends for illustrations

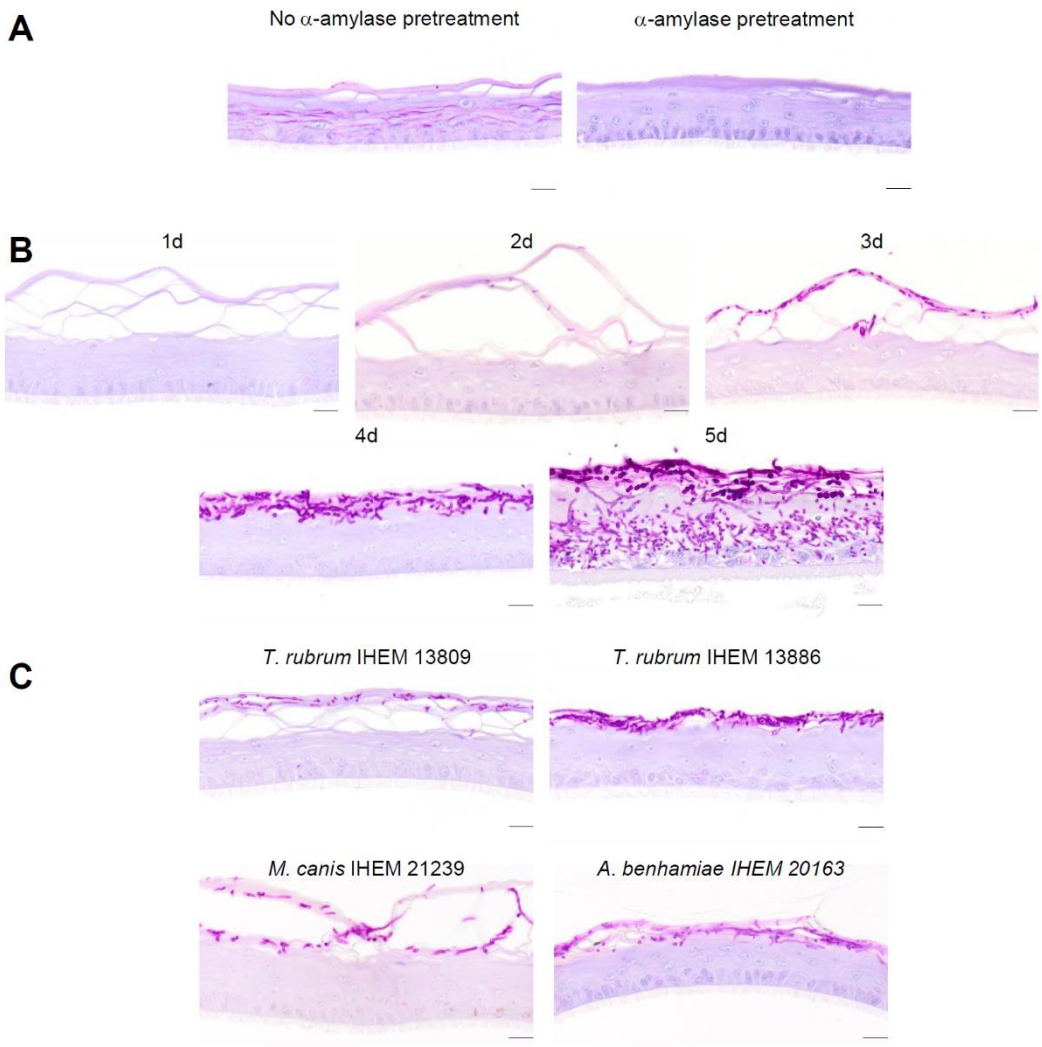

FIGURE 1: Infection of RHE using dermatophytes arthroconidia. Sections of non-infected control RHE at 11th day of reconstruction were histologically processed and stained by PAS with or without α-amylase pretreatment and with hemalun counterstaining. Prior digestion by α-amylase suppresses PAS signal in control RHE **(A)**. RHE infected by arthroconidia of *T. rubrum* IHEM 13894 at a density of 1,700 /cm² were processed for histological analysis and stained by PAS with α-amylase pretreatment and hemalun counterstaining, one (1d), two (2d), three (3d), four (4d) or five (5d) days after inoculation **(B)**. RHE infected by arthroconidia from two other strains of *T. rubrum*, namely IHEM 13809 or IHEM 13886 strain, at a density of 1,700 / cm², or by 17,000 arthroconidia of *M.* canis IHEM 21239 per cm² or by 53 arthroconidia of *A.*

benhamiae IHEM 20163 per cm² were processed for histological analysis four days after inoculation **(C)**. Scale bars: 20 µm.

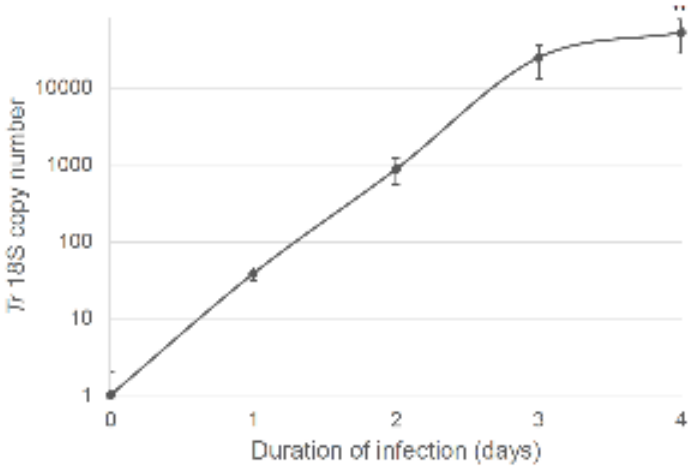

FIGURE 2: Infection of RHE is quantified by qPCR detection of *T. rubrum* 18S rDNA gene. RHE produced using keratinocytes from three different donors were infected by arthroconidia of *T. rubrum*. Each day during the four days following inoculation, DNA was extracted from infected RHE and *Tr* 18S rDNA copy number was determined by qPCR. DNA was also extracted from non-infected RHE before infection (0 day) and served as negative control (n=3 ± SD; **p<0.01; ANOVA1).

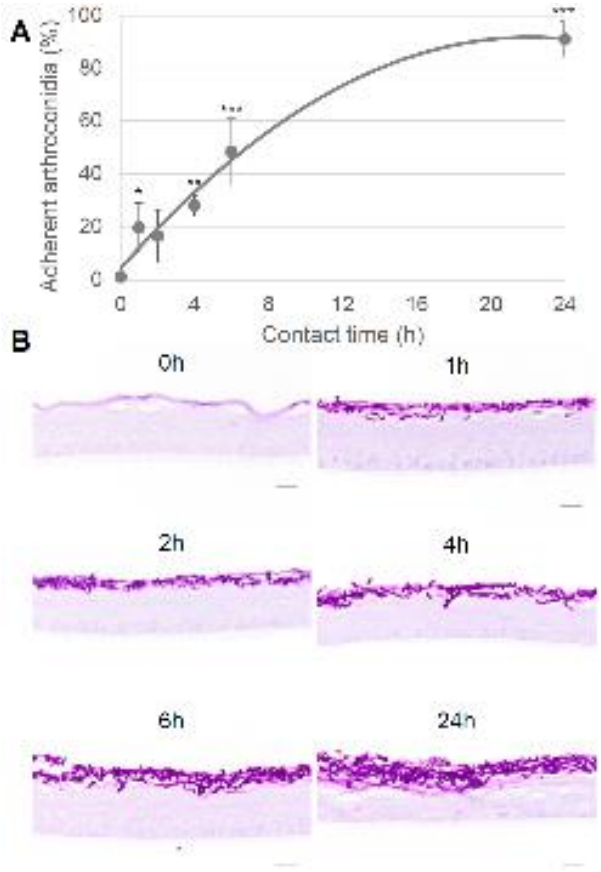

FIGURE 3: Adhesion kinetics of *T. rubrum* arthroconidia to RHE. RHE were infected by arthroconidia of *T. rubrum* (1,700/cm²). After 0, 1, 2, 4, 6 or 24h of contact time following inoculation, non-adherent arthroconidia were recovered by PBS washes and seeded on Sabouraud dextrose agar. Seven days later, CFU were counted and percentage of adherent arthroconidia was calculated. Statistical differences indicated on the graph were determined using RHE 0h as control (n=3 ± SD; *p<0.05 **p<0.01 ***p<0.001; ANOVA 1) **(A)**. Infected RHE were collected four days after inoculation, processed for histological analysis and stained by PAS with α-amylase pretreatment and hemalun counterstaining **(B)**. Scale bars: 20 µm.

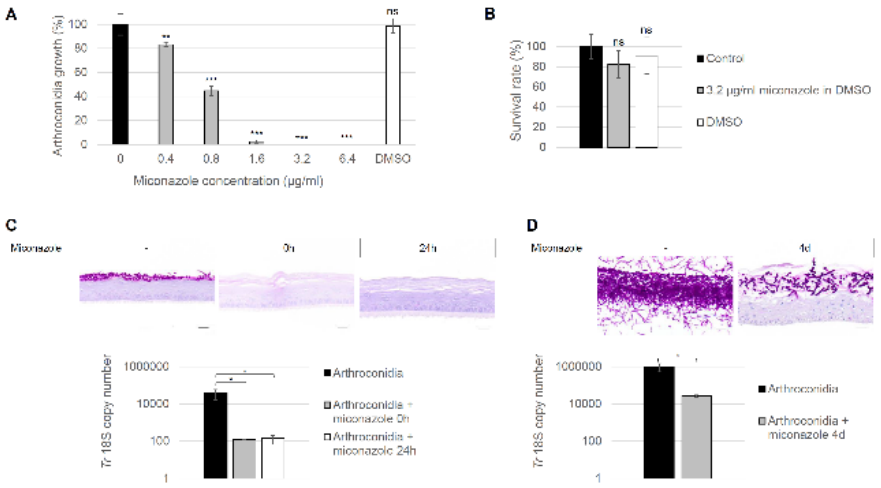

FIGURE 4: Inhibitory activity of miconazole on *T. rubrum* arthroconidia seeded on RHE.

Arthroconidia of *T. rubrum* were seeded on Sabouraud dextrose agar in presence of different concentrations of miconazole. Seven days later, CFU were counted and arthroconidia growth was evaluated: miconazole at a concentration of 3.2 µg/ml inhibits arthroconidia's growth (n=3 ± SD; $^{ns}p\geq0.05$ **p<0.01 ***p<0.01; ANOVA1) **(A)**. In addition, neither miconazole at this concentration nor DMSO, which is the solvent of miconazole, has significant effect on RHE survival as demonstrated by MTT assay (n=3 ± SD; $^{ns}p\geq0.05$; ANOVA1) **(B)**. RHE were infected by arthroconidia of *T. rubrum* only, or in presence of miconazole applied at the same time (0h) or applied 24h after infection (24h). Four days after inoculation, RHE were histologically processed and stained by PAS with α-amylase pretreatment and hemalun counterstaining **(C)**. Scale bars: 20 µm. Total DNA was extracted from RHE four days after inoculation with arthroconidia of *T. rubrum* only (arthroconidia), or in presence of miconazole applied at the same time (arthroconidia + miconazole 0h) or applied 24h after infection (arthroconidia + miconazole 24h). Measurement of *T. rubrum* 18S rDNA gene copy number was then performed by qPCR (n=3 ± SD; *p<0.05; ANOVA1) **(C)**. In a second experimental setting, RHE were infected by arthroconidia of *T. rubrum* only, or in presence of miconazole applied four days after infection (4d). Eight days after inoculation, RHE were histologically processed and

stained by PAS with α-amylase pretreatment and hemalun counterstaining **(D)**. Scale bars: 20 µm. Total DNA was extracted from RHE eight days after inoculation with arthroconidia of *T. rubrum* only (arthroconidia), or in presence of miconazole applied four days after infection (arthroconidia + miconazole 4d). Measurement of *T. rubrum* 18S rDNA gene copy number was then performed by qPCR (n=3 ± SD; *p<0.05; ANOVA1) **(D)**.